Myomerger induces fusion of non-fusogenic cells and is required for myoblast fusion

Malgorzata E. Quinn[1], Qingnian Goh[1], Mitsutoshi Kurosaka[1], Dilani G. Gamage[1], Michael J. Petrany[1], Vikram Prasad[1], Douglas P. Millay[1,*]

[1]Division of Molecular Cardiovascular Biology, Cincinnati Children's Hospital Medical Center, Cincinnati, OH 45229, USA.

*Corresponding author. E-mail: douglas.millay@cchmc.org

Abstract

Despite the importance of cell fusion for mammalian development and physiology, the factors critical for this process remain to be fully defined[1]. This lack of knowledge has severely limited our ability to reconstitute cell fusion, which is necessary to decipher the biochemical mechanisms driving plasma membrane merger. Myomaker (*Tmem8c*) is a muscle-specific protein required for myoblast fusion[2,3]. Expression of myomaker in fibroblasts drives their fusion with myoblasts, but not with other myomaker-fibroblasts, highlighting the requirement of additional myoblast-derived factors for fusion. Here, we demonstrate that *Gm7325*, named myomerger, induces the fusion of myomaker-expressing fibroblasts. Cell mixing experiments reveal that while myomaker renders cells fusion-competent, myomerger induces fusogenicity. Thus, myomaker and myomerger confer fusogenic activity to normally non-fusogenic cells. Myomerger is skeletal muscle-specific and only expressed during developmental and regenerative myogenesis. Disruption of myomerger in myoblast cell lines through Cas9-mutagenesis generated non-fusogenic myocytes. Genetic deletion of myomerger in mice results in a paucity of muscle fibers demonstrating a requirement for myomerger in normal muscle formation. Myomerger deficient myocytes exhibit an ability to differentiate and harbor organized sarcomeres, however remain mono-nucleated. These data identify myomerger as a fundamental myoblast fusion protein and establishes a system that begins to reconstitute mammalian cell fusion.

1 **Main**

2

3   The fusion of plasma membranes is necessary for numerous biological processes from

4   conception to the development of skeletal muscle, osteoclasts, trophoblasts, and giant cells.

5   The molecular regulation of fusion is poorly understood and the reconstitution of fusogenicity

6   has not been achieved in mammalian cells. Specifically, the factors that directly participate in

7   membrane coaelescence have not been identified.   The development of systems that

8   reconstitute fusion in the absence of other processes allow identification of nodal fusion

9   machinery and associated molecular mechanisms. For example, the *C. elegans* fusogen

10   epithelial fusion failure (Eff-1) is sufficient to fuse typically non-fusing cells[4,5] and mechanisms of

11   intracellular membrane fusion were partially revealed through reconstitution of SNAREs on

12   synthetic membranes[6-8]. Thus, discoveries of specific fusion proteins and development of

13   reconstitution systems have been historically critical to decipher multiple types of membrane

14   fusion, however these systems are lacking for mammalian cellular fusion.

15   Myoblast fusion is a highly specific process essential for muscle formation, and while

16   numerous proteins have been shown to regulate mammalian myoblast fusion[9-19], myomaker is

17   the only known muscle-specific protein absolutely required for this process[2]. Expression of

18   myomaker in fibroblasts or mesenchymal stromal cells (MSCs) induces their fusion with muscle

19   cells[20,21]. However, myomaker-fibroblasts do not fuse to each other indicating that additional

20   muscle-derived factors are required for fusion. To uncover potential factors, we compared genes

21   induced by expression of MyoD to their level of expression in 10T ½ fibroblasts. Of the top 100

22   MyoD-regulated genes not expressed in fibroblasts (Supplemental Information), we eliminated

23   genes not likely to be directly involved in fusion (transcription factors, sarcomeric and metabolic

24   genes) and focused on genes with transmembrane domains. This analysis yielded the following

25   five genes: *Tmem182, Gm7325, Cdh15, Tspan33*, and *Tm6sf1*, however *Cdh15* was omitted

26   from further analysis because it is not necessary for myoblast fusion or muscle formation[22]. We

27   retrovirally expressed each gene in myomaker$^+$ GFP$^+$ fibroblasts and assayed for fusion.

28   Appropriate expression in fibroblasts was verified through quantitative reverse transcription

29   polymerase chain reaction (qRT-PCR) analysis (Extended Data Fig. 1a). We observed mainly

30   mono-nucleated GFP$^+$ cells in all cultures except when *Gm7325* was expressed where

31   widespread multi-nucleated cells were present (Fig. 1a). Based on the ability of *Gm7325* to

32   induce fusion of myomaker$^+$ fibroblasts and the observations described below we named the

33   protein myomerger.

34   Multiple *Gm7325* transcripts are annotated in the University of California, Santa Cruz,

35   mouse genome. The shorter transcript contains a single exon and yields a protein with 84 amino

36   acids. In contrast, the longer transcript utilizes an upstream exon with an alternative start site

37   and results in a protein of 108 amino acids (Extended Data Fig. 2a). The single coding exon of

38   the short transcript is conserved in other mammalian genomes, including humans, while the

39   upstream alternative exon leading to the longer transcript is not highly conserved (Extended

40   Data Fig. 2b). For the initial screen we cloned the *Gm7325* locus into a retroviral vector, allowing

41   normal splicing and expression of both short and long transcripts. Transduction of myomaker$^+$

42   fibroblasts with either myomerger-short (S) or myomerger-long (L) induced formation of multi-

43   nucleated cells, indicating both proteins are sufficient for fusion (Extended Data Fig. 2c).

44   Additionally, myomerger and myomaker together induced fusion of 3T3 fibroblasts and MSCs

45   (Extended Data Fig. 2d), suggesting these two genes could activate fusion in a multitude of cell

46   types.

47   Given that multi-nucleated cells could arise from fusion or endoreplication, we designed

48   a system to validate that multi-nucleated cells observed in fibroblasts expressing both

49 myomerger and myomaker were generated through fusion. We engineered two fibroblast cell

50 lines that both express myomaker, with one expressing GFP and the other expressing nuclear-

51 localized TdTomato (NLS-Tom). Myomaker$^+$ GFP$^+$ and myomaker$^+$ NLS-Tom$^+$ fibroblasts were

52 infected with a myomerger retrovirus or a control empty retrovirus, mixed, and fusion was

53 assessed (Fig. 1b). We observed cells with multiple nuclei containing both GFP and NLS-Tom

54 in fibroblasts expressing myomaker and myomerger indicating fusion (Fig. 1b). Quantification

55 of fusion revealed approximately 20% of nuclei were contained in syncytia in cultures where

56 fibroblasts were expressing both myomaker and myomerger (Fig. 1b). These results confirm

57 that the observed syncytial cells are formed through fusion and that expression of myomaker

58 and myomerger is sufficient to confer fusogenicity in non-fusogenic fibroblasts.

59   We also sought to determine the cell biology of fusion induced by myomaker and

60 myomerger. We mixed myomaker$^+$ myomerger$^+$ GFP$^+$ fibroblasts with NLS-Tom$^+$ fibroblasts

61 expressing myomaker or myomerger (Extended Data Fig. 3). Here we observed fusion of

62 myomaker$^+$ myomerger$^+$ GFP$^+$ fibroblasts with myomaker$^+$ NLS-Tom$^+$ but not myomerger$^+$ NLS-

63 Tom$^+$ fibroblasts (Extended Data Fig. 3). This heterotypic nature of fibroblast fusion are

64 consistent with our previously reported heterologous fusion system between myoblasts and

65 fibroblasts[2]. In that system, myomaker$^+$ fibroblasts that did not express myomerger fused with

66 muscle cells, which express both myomaker and myomerger. We next utilized our heterologous

67 fusion system where fibroblasts were infected with GFP and either empty, myomaker, or

68 myomerger retrovirus, and then mixed with C2C12 myoblasts (Fig. 1c). In this assay, fusion is

69 detected through co-localization of GFP (fibroblasts) with myosin$^+$ myotubes. Compared to

70 empty-infected GFP$^+$ fibroblasts, we detected a significant increase in fusion between myosin$^+$

71 cells with either myomaker$^+$ GFP$^+$ fibroblasts or myomerger$^+$ GFP$^+$ fibroblasts (Fig. 1c). However,

72 quantification of myosin$^+$ GFP$^+$ cells revealed that myomerger did not drive the fusion of

73   fibroblasts with muscle cells to the levels observed with myomaker (Fig. 1c). These data confirm

74   myomaker is required in both fusing cells for *in vitro* fusion, while myomerger is essential in one

75   fusing cell.

76   The only current information regarding *Gm7325* is its potential expression in embryonic

77   stem (ES) cells[23], therefore we interrogated its expression pattern more thoroughly. We

78   performed qRT-PCR on multiple tissues from postnatal (P) day 5 mice with primers to distinguish

79   the two potential mouse transcripts (Extended Data Fig. 4a). In neonatal tissues, we detected

80   expression of both myomerger transcripts only in skeletal muscle (Fig. 2a). Despite the evidence

81   of two myomerger transcripts, immunoblot analysis of skeletal muscle lysates from P5 mice

82   using a commercially available antibody identified a single band at approximately 12 kDa. This

83   band was absent in P28 lysates indicating that myomerger is downregulated after neonatal

84   development (Fig. 2b). Skeletal muscle exhibits a robust ability to regenerate due to the

85   presence of muscle stem cells, also known as satellite cells[24,25]. We analyzed expression of

86   myomerger in mdx^{4cv} mice, which is a mouse model of muscular dystrophy that leads to chronic

87   cycles of degeneration and regeneration[26]. Myomerger expression was detected in diaphragm

88   lysates from mdx^{4cv} mice, but not control diaphragms (Fig. 2c). Finally, we analyzed expression

89   of myomerger in a model of skeletal muscle overload-induced (MOV) hypertrophy and observed

90   up-regulation (Fig. 2d). Collectively, these data demonstrate that myomerger is expressed only

91   during development and is induced upon satellite cell activation in the adult.

92   We next sought to determine if myomerger is regulated as myoblasts differentiate. In

93   C2C12 cells, both *Gm735* transcripts were significantly elevated during differentiation (Extended

94   Data Fig. 4b). Similarly, myomerger protein levels were low in proliferating myoblasts (day 0),

95   but increased upon differentiation with expression maintained during myoblast differentiation and

96   fusion into myotubes (Fig. 2e). The short mouse myomerger protein, but not the long form, is

97   highly conserved among vertebrate species (Extended Data Fig. 4c).   After transduction of

98   C2C12 cells with empty, myomerger-S, or myomerger-L we detected an increased upper band

99   in cells expressing either myomerger-S or myomerger-L that co-migrated with the 12 kDa

100   endogenous protein in the empty-infected C2C12 cells (Extended Data Fig. 4d).   A lower band

101   was identified exclusively in myomerger-S lysates suggesting that complex mRNA or post-

102   translational processing results in the endogenous single 12 kDa band observed in WT C2C12

103   cells and muscle homogenates. Both myomerger proteins harbor a hydrophobic region close to

104   the N-terminus, where computational analysis of this region indicates a signal peptide or

105   transmembrane domain (Extended Data Fig. 4e). Given that both variants were found to confer

106   fusogenicity, the significance of the predicted domains is presently unclear.   To understand

107   subcellular localization, we fractionated C2C12 cells on day 2 of differentiation and identified

108   myomerger in membrane fractions containing caveolin-3, a protein known to associate with both

109   heavy and light vesicles (Fig. 2f).   Immunostaining of fibroblasts expressing myomerger-S or

110   myomerger-L shows that both proteins exhibit similar diffuse and vesicular localization (Fig. 2g).

111   Thus, myomerger associates with membrane compartments consistent with its ability to induce

112   fusion.

113   The ability of myomerger to induce fusion of myomaker-fibroblasts, and its muscle-

114   specific expression in the mouse, suggests that myomerger may play a critical role during

115   myogenesis.   To begin to decipher the role of myomerger in myogenesis, we evaluated its

116   function during myoblast differentiation. We utilized CRISPR/Cas9 genome editing to disrupt

117   myomerger in C2C12 myoblasts.   Two guide RNAs (gRNA) were designed to target the largest

118   exon of *Gm7325*, which resulted in a 166 base pair deletion thereby disrupting both mouse

119   transcripts (Extended Data Fig. 5a).   C2C12 cells were transfected with a plasmid containing

120   Cas9 with an IRES-GFP and myomerger gRNAs, or transfected with only Cas9-IRES-GFP as a

121   control. Flow cytometry of GFP$^+$ cells followed by genotyping through PCR analysis revealed

122   disruption of the myomerger locus (Extended Data Fig. 5b). Myomerger was not detectable in

123   myomerger KO C2C12 cells confirming efficient disruption of the locus (Fig. 3a). Control and

124   myomerger KO C2C12 cells were then analyzed for their ability to differentiate and form

125   myotubes. WT myoblasts differentiated, as indicated by myosin$^+$ cells, and fused to form multi-

126   nucleated myotubes (Fig. 3b). In contrast, myomerger KO C2C12 cells exhibited the ability to

127   differentiate but lacked fusogenic activity to form myotubes (Fig. 3b). Indeed, quantification of

128   the differentiation index revealed no difference in the percentage of myosin$^+$ cells between WT

129   and myomerger KO cultures (Fig. 3c). Additionally, quantification of fusion demonstrated that

130   myomerger KO myosin$^+$ cells remain mono-nucleated while WT cells fuse (Fig. 3d). qRT-PCR

131   analysis for the myogenic genes *Myogenin*, *Myh4*, *Ckm*, and *Tmem8c* (myomaker) further

132   indicated that myomerger KO myoblasts activate the differentiation program (Fig. 3e).

133   Interestingly, myogenic transcripts were elevated in myomerger KO cells potentially suggesting

134   a feedback mechanism by which non-fusogenic cells attempt to further differentiate (Fig. 3e).

135   Infection of myomerger KO C2C12 cells with either myomerger-S or myomerger-L rescued the

136   fusion defect demonstrating that the phenotype in these cells is specifically due to the loss of

137   myomerger (Extended Data Fig. 5c). Western blot analysis from these lysates shows re-

138   expression of myomerger in KO cells (Extended Data Fig. 5d). As a potential mechanism for the

139   lack of fusion in myomerger KO myocytes, we examined expression and localization of

140   myomaker. On day 2 of differentiation, myomerger KO cells exhibited normal expression and

141   localization of myomaker (Extended Data Fig. 6a). Moreover, we did not detect widespread co-

142   localization between myomaker and myomerger suggesting that myomerger does not directly

143   regulate myomaker distribution (Extended Data Fig. 6b). These data reveal that myomerger is

144   necessary for myoblast fusion *in vitro*.

145   To examine the function of myomerger *in vivo*, we disrupted exon 3 using the same

146   CRISPR/Cas9 strategy described for C2C12 myoblasts. Injection of Cas9 and myomerger

147   gRNAs into blastocysts resulted in lethality of 9 of the 10 F_0 pups, suggesting that the high

148   efficiency of Cas9 lead to homozygous deletion of myomerger. The one remaining pup was

149   heterozygous for myomerger and was mated to generate $Gm7325^{-/-}$ mice (Extended Data Fig.

150   7a). Sequencing the mutant PCR product from the heterozygous founder revealed the presence

151   of the same mutation as was achieved in C2C12 cells. We failed to observe any $Gm7325^{-/-}$ mice

152   upon genotyping two litters at P7 suggesting that, in conjunction with the lethality detected

153   through initial generation of F_0 pups, myomerger is essential for life. Indeed, E17.5 $Gm7325^{-/-}$

154   embryos exhibited minimal skeletal muscle upon gross examination (Fig. 4a). Specifically, bones

155   of the limbs and rib cage were noticeable due to a scarcity of surrounding muscle as observed

156   in WT embryos. Myomerger KO mice also display a hunched appearance with elongated snouts,

157   hallmark characteristics in embryos with improper muscle formation (Fig. 4a). Detection of

158   myomerger by western blot of WT and $Gm7325^{-/-}$ tongues showed elimination of myomerger

159   protein in KO samples (Extended Data Fig. 7b). E15.5 forelimb sections show that myomerger

160   KO myoblasts express myogenin indicating that specification and differentiation are activated

161   despite loss of myomerger (Fig. 4b). Moreover, histological analysis of multiple muscle groups

162   at E15.5 revealed the presence of myosin$^+$ muscle cells and sarcomeric structures in myomerger

163   KO mice, (Fig. 4c and Extended Data Fig. 7c). While multi-nucleated myofibers were present in

164   WT mice, these structures were not readily detected in myomerger KO mice indicating that

165   genetic loss of myomerger renders myocytes non-fusogenic (Fig. 4c and Extended Data Fig. 7c).

166   Analysis of forelimbs from E17.5 WT and myomerger KO embryos confirm that myomerger KO

167   myoblasts are unable to properly fuse, although we did detect myocytes with two nuclei

168   (Extended Data Fig. 7d-f). These results, together with our *in vitro* analysis, reveals that

169   myomerger is required for muscle formation during mammalian development through regulation

170   of myoblast fusion.

171   In summary, we report the discovery of an additional muscle-specific factor required for

172   myoblast fusion and developmental myogenesis. While myomaker and myomerger are both

173   necessary for muscle formation, E17.5 myomerger KO embryos exhibit more myocytes

174   compared to embryos lacking myomaker suggesting that these two key myoblast fusion proteins

175   may have distinct functions. Given that myomaker and myomerger are both essential for

176   myoblast fusion, an understanding of their precise function will aid in the delineation of

177   mammalian plasma membrane fusion mechanisms. The fibroblast cell fusion system developed

178   here, through expression of myomaker and myomerger, provides a unique platform to decipher

179   fusion mechanisms. Moreover, the induction of cell fusion by two factors represents an avenue

180   for gene delivery to potentially any tissue.

181

182 **Methods**

183

184 **Cell Culture**

185 C2C12 cells, 10T 1/2 fibroblasts, and NIH/3T3 fibroblasts were purchased from American Type

186 Culture Collection and propagated in DMEM (Gibco) containing 10% heat-inactivated bovine

187 growth serum (BGS) and supplemented with antibiotics. C2C12 cells were differentiated by

188 switching to media containing 2% heat-inactivated horse serum (HS) and antibiotics. MSCs

189 were a gift from Jose Cancelas and described previously[27].

190

191 **Bioinformatic Analysis**

192 Microarray data from the GEO DataSet GSE34907[28] was interrogated using GEO2R analysis to

193 identify 1826 genes displaying an increase greater than 1 log fold-change in MyoD-expressing

194 fibroblasts. In parallel, a transcriptional profile of 10T 1/2 fibroblasts transduced with empty virus

195 was generated using RNA-seq analysis (paired-end library layout using Illumina sequencing

196 platform) and a list of all genes with RPKM values below 1.5 compiled using Strand NGS

197 software (Ver. 2.6; Build: Mouse mm10 (UCSC) using Ensembl transcript annotations). These

198 two gene lists were then compared to generate a final tally comprised of 531 genes that were

199 both upregulated in MyoD-expressing fibroblasts and had low or no detectable expression in

200 10T 1/2 fibroblasts. Finally, the top 100 genes were interrogated for genes that contain

201 transmembrane domains and not previously studied for their role during myoblast fusion.

202

203 **Animals**

204 We used a dual sgRNA targeting strategy to create $Gm7325^{-/-}$ mice. We selected the sgRNAs

205 according to the on- and off-target scores from the web tool CRISPOR[29]. The selected gRNAs

206   were 5'-GCAGCGATCGAAGCACCATC-3' and 5'-GAGGCCTCTCCAGAATCCGG-3' that target

207   exon 3 of *Gm7325*. The sgRNAs were *in vitro* synthesized using the MEGAshortscript T7 kit

208   (ThermoFisher) and purified by the MEGAclear Kit (ThermoFisher), as previously described[30].

209   sgRNAs (50 ng/ul of each) were mixed with 100 ng/ul Cas9 protein (ThermoFisher) and

210   incubated at 37°C for 15 min to form a ribonucleoprotein complex. We then injected the mix into

211   the cytoplasm of one-cell-stage embryos of the C57BL/6 genetic background using a piezo-

212   driven microinjection technique as described previously[30]. Injected embryos were immediately

213   transferred into the oviducal ampulla of pseudopregnant CD-1 females. Live born pups were

214   genotyped by PCR with the following primers: F: 5′- GAAGGGAGGACTCCACACCC-3' and R:

215   5'-CGCCTGGACTAACCGGCTCC-3'. The edited allele was further confirmed by Sanger

216   sequencing. One heterozygous founder was obtained and mated with WT C57Bl6 mice to

217   eventually generate KO mice. Mdx^{4cv} mice were purchased from Jackson Laboratory (#002378).

218   Muscle overload of the plantaris muscle was achieved through bilateral synergistic ablation of

219   soleus and gastrocnemius muscles as described by others[31]. Briefly, the soleus and

220   gastrocnemius muscles were exposed by making an incision on the posterior-lateral aspect of

221   the lower limb. The distal and proximal tendons of the soleus, lateral and medial gastrocnemius

222   were subsequently cut and carefully excised. All animal procedures were approved by Cincinnati

223   Children's Hospital Medical Center's Institutional Animal Care and Use Committee.

224

225   **CRISPR-Mediated Genome Editing in C2C12 Cells**

226   Freshly plated low passage C2C12 cells were transfected with 4µg of a modified pX458 plasmid

227   (Addgene #48138, gift from Yueh-Chiang Hu), which contained a high fidelity Cas9, an optimized

228   sgRNA scaffold, and an IRES-GFP cassette. The same gRNAs used to generate KO animals

229   were used for C2C12 cells. 16 µL of Lipofectamine 2000 was used for this transfection. 5×10^{5}

230   C2C12 cells were transfected in a 60 mm culture dish. Forty-eight hours after transfection GFP$^+$

231   cells were sorted into 96 well plates using FACS. These cells were maintained in DMEM

232   containing 20% FBS with antibiotics at subconfluent densities. The cell lines were genotyped by

233   amplifying a 420 bp region surrounding the site of Cas9 activity using the primers used to

234   genotype *Gm7325*$^{-/-}$ animals.

235

236   **Cloning and viral infection**

237   We initially cloned a region of the *Gm7325* locus, containing all genomic information for

238   expression of myomerger-short and myomerger-long, from C57Bl6 mouse genomic DNA using

239   the following primers: F: 5'-AGTGATGCTGAATCCACCGCA-3' and R: 5'-

240   CCAATAACAACACACTGTCCT-3'. We cloned myomerger-short and long coding sequences

241   from cDNA of differentiating C2C12 cells using the following primers: myomerger-long F: 5'-

242   ATGCCAGAAGAAAGCTGCACTG-3', myomerger-short F: 5'-

243   ATGCCCGTTCCATTGCTCCCGA-3', and a common myomerger R: 5'-TCA CTT CTG GGG

244   GCC CAA TCT C-3'. Myomerger cDNA and genomic DNA was cloned into the retroviral vector

245   pBabe-X[2] using EcoRI. Myomaker and GFP retroviral plasmids have been described previously[2].

246   NLS-TdTomato was subcloned from pQC-NLS-TdTomato (Addgene #37347) into the retroviral

247   vector pMX (Cell Biolabs). Plasmids containing cDNA for Tmem182, Tspan33, and Tm6sf1 from

248   the Mammalian Gene Collection were purchased from Open Biosystems and subcloned into

249   pBabe-X. Ten micrograms of retroviral plasmid DNA were transfected with FuGENE 6 (Roche)

250   into Platinum E cells (Cell Biolabs), which were plated 24 hours before transfection on a 10 cm

251   culture dish at a density of 3-4x10^6 cells per dish. Forty-eight hours after transfection, viral media

252   were collected, filtered through a 0.45 μm cellulose syringe filter and mixed with polybrene

253   (Sigma) at a final concentration of 6 μg/ml. Target cells were plated on 10 cm culture dishes at

254 a density of 4×10^5 cells per dish 16-18 hours before infection. Eighteen hours after infection,

255 virus was removed, cells were washed with PBS and split into new 10 cm dishes.

256

Cell fusion assays

258 Cells were split 18 hours after retroviral infection and split again 24-48 hours later. At the second

259 split, cells were seeded for the fusion assay on 35-mm dishes ($3-4\times10^5$ cells per dish) or on 8-

260 well Ibidi slides (2×10^4 cells/well). Fusion was assessed 24-48 hours after seeding. For

261 heterologous fusion, cultures of fibroblasts and myoblasts mixed at a ratio of 1:1 (1.5×10^5 cells

262 for each) were induced to differentiate 24 hours after seeding and fusion was assessed on day

263 4 of differentiation.

264

RNA extraction and quantitative RT-PCR (qRT-PCR)

266 Total RNA was extracted from either mouse tissue or cultured cells with TRIZOL (Life

267 Technologies) according to manufacturer's protocol. cDNA was synthesized using High-

268 Capacity cDNA Reverse Transcription Kit (Applied Biosystems) with random primers. Gene

269 expression was assessed using standard quantitative PCR approach with Power Sybr® Green

270 PCR mastermix (Applied Biosystems). Analysis was performed on StepOnePlus Real-Time PCR

271 system (Applied Biosystems) with the following primers: myomerger-short-F: 5′-

272 CAGGAGGGCAAGAAGTTCAG-3′ and myomerger-R: 5′-ATGTCTTGGGAGCTCAGTCG-3′;

273 myomerger-long-F: 5′-ACCAGCTTTCATGCCAGAAG-3′ and myomerger-R: 5′-

274 ATGTCTTGGGAGCTCAGTCG-3′; myomaker-F: 5′-ATCGCTACCAAGAGGCGTT-3′ and

275 myomaker-R: 5′-CACAGCACAGACAAACCAGG-3′; Tm6sf1 F: 5'-

276 TTAGTGGTCCCTGGATGCTC-3" and Tm6sf1 R: 5'-GACGCACCAATGTGAGAAAA-3';

277 Tspan33-F: 5'-GGGGACGAGTTCTCCTTCG-3' and Tspan33 R: 5'-

278   TGCTTCTGCGTGCTTCATTAG-3'; Tmem182-F: 5'-GGCTCTCTTCGGAGCTTTGG-3' and

279   Tmem182-R: 5'-GGTGGCTGATTGGTGTACCAG-3';   myogenin-F: 5'-

280   CTACAGGCCTTGCTCAGCTC-3' and myogenin-R: 5'-GTGGGAGTTGCATTCACTGG-3';

281   Ckm-F: 5'-ACCTCCACAGCACAGACAGA-3' and Ckm-R: 5'-CAGCTTGAACTTGTTGTGGG-3';

282   Myh4-F: 5'-GCAGGACTTGGTGGACAAAC-3' and Myh4-R: 5'-ACTTGGCCAGGTTGACATTG-

283   3';   GAPDH-F: 5'-TGCGACTTCAACAGCAACTC-3'   and   GAPDH-R: 5'-

284   GCCTCTCTTGCTCAGTGTCC-3'.

285

286   **Western blot analysis**

287   Cultured cells were washed two times with ice cold PBS, scraped into a conical tube, pelleted,

288   resuspended in lysis buffer (50 mM Tris-HCl, pH 6.8, 1mM EDTA, 2% SDS) and sonicated for a

289   total of 15 seconds (three 5 second pulses). Skeletal muscle tissues from mice were

290   homogenized with a bead homogenizer (TissueLyser II; Qiagen) in lysis buffer (10 mM Tris (pH

291   7.4), 1 mM EDTA, 1mM dithiothreitol, 0.5% Triton X-100, 2.1 mg/ml NaF) containing protease

292   and phosphatase inhibitor cocktails (5 µl/ml; Sigma-Aldrich). Both cells and tissue lysates were

293   centrifuged to pellet insoluble material and protein concentration was determined using Bradford

294   protein assay. Equal amounts of protein (5 µg for cells and 20 µg for tissues) were prepared with

295   loading buffer (1x Laemmli (Bio-Rad) with reducing agent (5% β-mercaptoethanol for cells and

296   100 mM DTT for tissues). Samples were heated at 37°C for 30 minutes and separated on a 20%

297   SDS-PAGE. The gels were subsequently transferred to a PVDF membrane (Millipore), blocked

298   in 5% milk in Tris-buffered saline/0.1% Tween-20 (TBS-T) and incubated with anti-sheep ESGP

299   antibody (1 mg/µl; R&D Systems) overnight at 4°C. Membranes were then washed with TBS-T

300   and incubated with Alexa-Fluor 647 donkey anti-sheep secondary antibody (1:5,000; Invitrogen).

301   Bands were visualized using the Odyssey® infrared detection system (LI-COR Biosciences).

302   GAPDH (1:5,000; Millipore) was used as a loading control.

303

Subcellular fractionation

305   C2C12 cells were harvested on day 2 of differentiation in ice cold hypotonic buffer (10 mM Tris-

306   HCl pH 8, 2 mM EDTA) and lysed using a dounce homogenizer. Lysates were then centrifuged

307   at 800 x g for 5 mintues at 4°C to separate nuclei and cell debris. That supernatant was then

308   centrifuged at 5000 x g for 10 minutes to pellet mitochondria and ER. ER and heavy vesicles

309   were further pelleted through centrifugation at 17,000 x g for 10 minutes. Finally, plasma

310   membrane, light vesicles, and organelles were pelleted at 100,000 x g for 20 minutes and the

311   supernatant from this spin was collected as the cytosolic fraction. All pellets were resuspended

312   in lysis buffer (50 mM Tris-HCl, pH 6.8, 1mM EDTA, 2% SDS) at volumes equal to the

313   supernatant. 8 μl of each fraction was separated by SDS-PAGE and analyzed for presence of

314   myomerger, caveolin-3, and tubulin. Caveolin-3 antibody (BD Transduction Laboratories

315   #610421) was used at 1:6700 and tubulin (Santa Cruz #SC-8035) at 1:50.

316

Immunocytochemistry

318   Cultured cells were rinsed with PBS and fixed in 4% paraformaldehyde (PFA)/PBS for 15

319   minutes at room temperature. Cells were subsequently permeabilized and blocked in 0.01%

320   Triton X-100/5% donkey serum/PBS for one hour at room temperature. Primary antibody diluted

321   in permeabilization/blocking buffer was incubated overnight. Cells were then washed with PBS

322   and incubated with secondary Alexa-Fluor antibodies (1:250) for 1 hour. A myomaker antibody

323   custom antibody was generated through YenZym Antibodies LLC. Rabbits were immunized with

324   amino acids #137-152 of mouse myomaker (MKEKKGLYPDKSIYTQ) after conjugation to KLH.

325   We used antigen-specific affinity purified products at a concentration of 4.3 μg/mL for

326   immunostaining. Esgp (myomerger) antibody was used at a concentration of 1 μg/mL. Anti-

327   mouse myosin (my32, MA5-11748, ThermoFisher Scientific) antibody was used at 1:100.

328   Hoechst 33342 solution (ThermoFisher Scientific) was used to stain nuclei. Cells were imaged

329   using Nikon A1R+ confocal on a FN1 microscope (35 mm dishes) or Nikon A1R confocal on

330   Eclipse T1 inverted microscope (Ibidi slides).

331

332   **Histology and immunohistochemistry**

333   For cryosections, embryos were dissected, fixed in 4% PFA/PBS overnight at 4°C, washed in

334   PBS, incubated in 30% sucrose/PBS overnight and then in 1:1 mix of optimal cutting temperature

335   (O.C.T.) formulation and 30% sucrose prior to embedding in O.C.T.. Sections were cut at 10 μm

336   and then permeabilized with 0.2% Triton X-100/PBS, blocked with 1% BSA/1% heat inactivated

337   goat serum/0.025% Tween20/PBS and incubated with primary antibody overnight. Anti-mouse

338   myosin (my32, MA5-11748, ThermoFisher Scientific) antibody was used at 1:100, whereas

339   myogenin (F5D, Developmental Hybridomas) was used at a concentration of 2.56 μg/mL.

340   Secondary goat anti-mouse IgG1-488 Alexa-Fluor antibody (Invitrogen) was incubated at a

341   dilution of 1:250 for 1 hour. Slides were mounted with VectaShield containing DAPI (Vector

342   Laboratories) and visualized using Nikon A1R confocal on Eclipse T1 inverted microscope.

343   Images were analyzed with Fiji.

344

345   **Statistical analysis**

346   For quantitation of cell fusion in Fig. 1b, cells with 3 or more nuclei were considered syncytial

347   cells. The number of nuclei in syncytial cells and total number of nuclei were manually counted.

348   In Fig. 1c, the number of myosin[+] myotubes (myosin structures with 3 or more nuclei) and GFP[+]

349   myosin$^+$ myotubes were manually counted. To quantify fusion between myomaker$^+$ myomerger$^+$

350   GFP$^+$ fibroblasts with either myomaker$^+$ NLS-Tom$^+$ or myomerger$^+$ NLS-Tom$^+$ fibroblasts

351   (Extended Data Fig. 3), we calculated the percentage of GFP$^+$ NLS-Tom$^+$ syncytial cells. The

352   differentiation index (Fig. 3c) was calculated as the percentage of nuclei in myosin$^+$ cells, and

353   the fusion index (Fig. 3d) as the percentage of myosin$^+$ cells with the indicated number of nuclei.

354   Quantitative data sets are presented as means ± SEM. For each quantitiation, at least 3

355   independent experiments were performed in duplicate and 4-6 fields were randomly chosen for

356   imaging. Histological analysis of embryos was performed on 3-4 embryos per genotype per time

357   point. Multiple histological levels within each muscle were examined. The data were analyzed

358   using an unpaired Student's t-test with GraphPad Prism 6 software. A value of $P < 0.05$ was

359   considered statistically significant.

360

365

366   **Author Contributions** D.P.M and M.E.Q. designed and performed experiments, and analyzed

367   the data. Q.G., M.K., D.G.G., M.J.P., and V.K. performed experiments. D.P.M. wrote the

368   manuscript with assistance from all authors.

369

370   **Author Information** The authors declare no competing financial interests. Correspondence and

371   requests for materials should be addressed to D.P.M. (douglas.millay@cchmc.org).

372

References

1   Kim, J. H., Jin, P., Duan, R. & Chen, E. H. Mechanisms of myoblast fusion during muscle development. *Curr Opin Genet Dev* **32**, 162-170, (2015).

2   Millay, D. P. *et al.* Myomaker is a membrane activator of myoblast fusion and muscle formation. *Nature* **499**, 301-305, (2013).

3   Millay, D. P., Sutherland, L. B., Bassel-Duby, R. & Olson, E. N. Myomaker is essential for muscle regeneration. *Genes Dev* **28**, 1641-1646, (2014).

4   Podbilewicz, B. *et al.* The c. Elegans developmental fusogen eff-1 mediates homotypic fusion in heterologous cells and in vivo. *Dev Cell* **11**, 471-481, (2006).

5   Shilagardi, K. *et al.* Actin-propelled invasive membrane protrusions promote fusogenic protein engagement during cell-cell fusion. *Science* **340**, 359-363, (2013).

6   Ohya, T. *et al.* Reconstitution of rab- and snare-dependent membrane fusion by synthetic endosomes. *Nature* **459**, 1091-1097, (2009).

7   Ma, C., Su, L., Seven, A. B., Xu, Y. & Rizo, J. Reconstitution of the vital functions of munc18 and munc13 in neurotransmitter release. *Science* **339**, 421-425, (2013).

8   Weber, T. *et al.* Snarepins: Minimal machinery for membrane fusion. *Cell* **92**, 759-772, (1998).

9   Horsley, V., Jansen, K. M., Mills, S. T. & Pavlath, G. K. Il-4 acts as a myoblast recruitment factor during mammalian muscle growth. *Cell* **113**, 483-494, (2003).

10   Hamoud, N., Tran, V., Croteau, L. P., Kania, A. & Cote, J. F. G-protein coupled receptor bai3 promotes myoblast fusion in vertebrates. *Proc Natl Acad Sci U S A* **111**, 3745-3750, (2014).

11   Laurin, M. *et al.* The atypical rac activator dock180 (dock1) regulates myoblast fusion in vivo. *Proc Natl Acad Sci U S A* **105**, 15446-15451, (2008).

12   Leikina, E. *et al.* Extracellular annexins and dynamin are important for sequential steps in myoblast fusion. *J Cell Biol* **200**, 109-123, (2013).

13   Vasyutina, E., Martarelli, B., Brakebusch, C., Wende, H. & Birchmeier, C. The small g-proteins rac1 and cdc42 are essential for myoblast fusion in the mouse. *Proc Natl Acad Sci U S A* **106**, 8935-8940, (2009).

14   Redelsperger, F. *et al.* Genetic evidence that captured retroviral envelope syncytins contribute to myoblast fusion and muscle sexual dimorphism in mice. *PLoS Genet* **12**, e1006289, (2016).

15   Nowak, S. J., Nahirney, P. C., Hadjantonakis, A. K. & Baylies, M. K. Nap1-mediated actin remodeling is essential for mammalian myoblast fusion. *J Cell Sci* **122**, 3282-3293, (2009).

16   Park, S. Y. *et al.* Stabilin-2 modulates the efficiency of myoblast fusion during myogenic differentiation and muscle regeneration. *Nat Commun* **7**, 10871, (2016).

17   Webster, M. T. & Fan, C. M. C-met regulates myoblast motility and myocyte fusion during adult skeletal muscle regeneration. *PLoS One* **8**, e81757, (2013).

18   Schwander, M. *et al.* Beta1 integrins regulate myoblast fusion and sarcomere assembly. *Dev Cell* **4**, 673-685, (2003).

19   Demonbreun, A. R., Biersmith, B. H. & McNally, E. M. Membrane fusion in muscle development and repair. *Semin Cell Dev Biol* **45**, 48-56, (2015).

20   Millay, D. P. *et al.* Structure-function analysis of myomaker domains required for myoblast fusion. *Proc Natl Acad Sci U S A* **113**, 2116-2121, (2016).

21   Mitani, Y., Vagnozzi, R. J. & Millay, D. P. In vivo myomaker-mediated heterologous fusion and nuclear reprogramming. *FASEB J* **31**, 400-411, (2017).

420   22   Hollnagel, A., Grund, C., Franke, W. W. & Arnold, H. H. The cell adhesion molecule m-
421   cadherin is not essential for muscle development and regeneration. *Mol Cell Biol* **22**,
422   4760-4770, (2002).
423   23   Chen, Y. M., Du, Z. W. & Yao, Z. Molecular cloning and functional analysis of esgp, an
424   embryonic stem cell and germ cell specific protein. *Acta Biochim Biophys Sin (Shanghai)*
425   **37**, 789-796, (2005).
426   24   Chang, N. C. & Rudnicki, M. A. Satellite cells: The architects of skeletal muscle. *Curr Top*
427   *Dev Biol* **107**, 161-181, (2014).
428   25   Montarras, D., L'Honore, A. & Buckingham, M. Lying low but ready for action: The
429   quiescent muscle satellite cell. *FEBS J* **280**, 4036-4050, (2013).
430   26   Durbeej, M. & Campbell, K. P. Muscular dystrophies involving the dystrophin-glycoprotein
431   complex: An overview of current mouse models. *Curr Opin Genet Dev* **12**, 349-361,
432   (2002).
433   27   Gonzalez-Nieto, D. *et al.* Connexin-43 in the osteogenic bm niche regulates its cellular
434   composition and the bidirectional traffic of hematopoietic stem cells and progenitors.
435   *Blood* **119**, 5144-5154, (2012).
436   28   Fong, A. P. *et al.* Genetic and epigenetic determinants of neurogenesis and myogenesis.
437   *Dev Cell* **22**, 721-735, (2012).
438   29   Haeussler, M. *et al.* Evaluation of off-target and on-target scoring algorithms and
439   integration into the guide rna selection tool crispor. *Genome Biol* **17**, 148, (2016).
440   30   Yang, H., Wang, H. & Jaenisch, R. Generating genetically modified mice using crispr/cas-
441   mediated genome engineering. *Nat Protoc* **9**, 1956-1968, (2014).
442   31   Dearth, C. L. *et al.* Skeletal muscle cells express icam-1 after muscle overload and icam-
443   1 contributes to the ensuing hypertrophic response. *PLoS One* **8**, e58486, (2013).
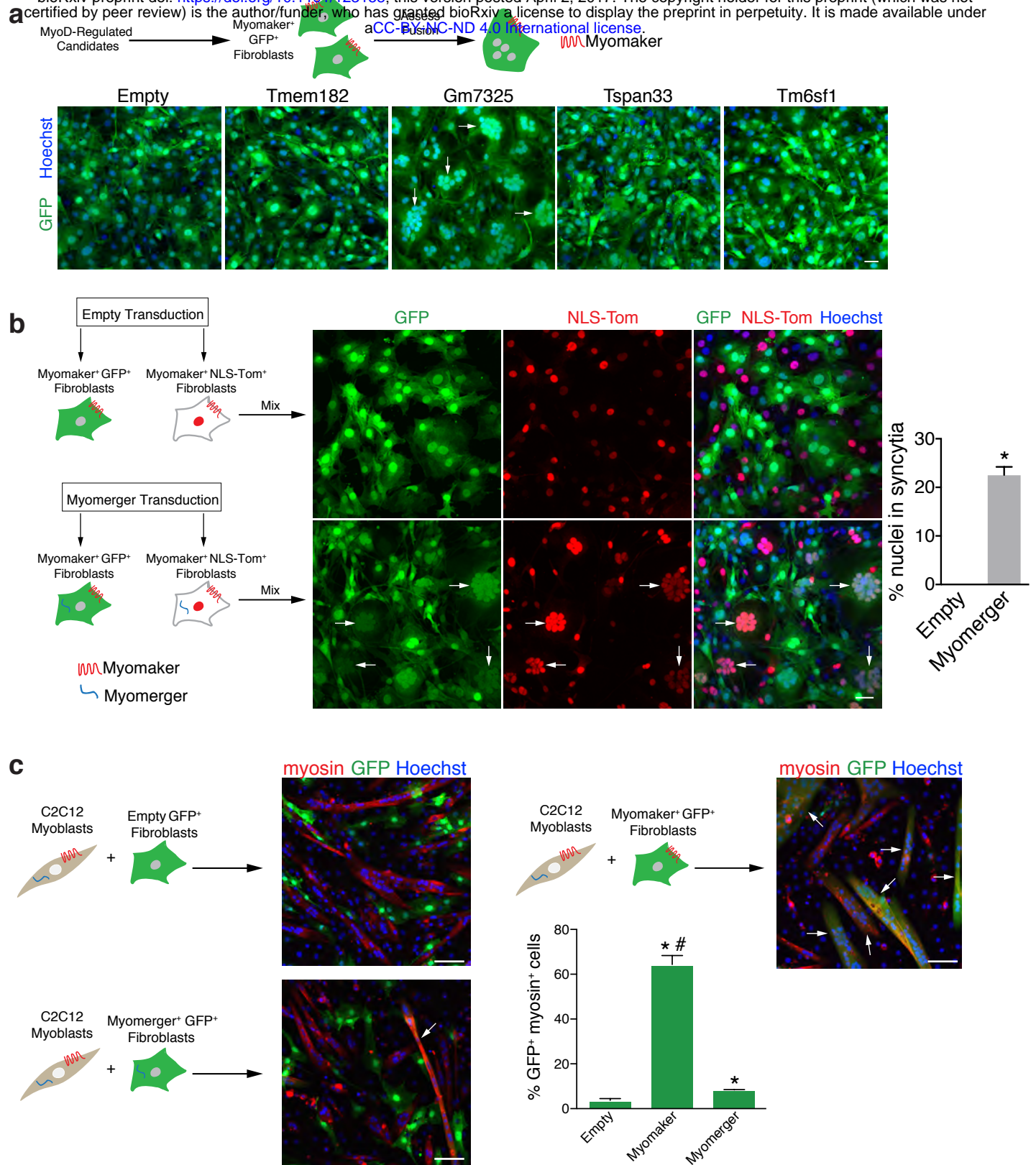444

Figure 1. Induction of fibroblast fusion by myomerger. a, Schematic showing a screen for muscle genes that could activate fusion of GFP+ myomaker+ fibroblasts. Representative images of GFP+ cells and nuclei after expression of the indicated genes. Arrows depict cells with multiple nuclei. **b**, Illustration of cell mixing approach to show fusion between the populations of fibroblasts. Co-localization of GFP and NLS-TdTomato (NLS-Tom) in the nucleus represents fusion. Representative images demonstrate fusion of myomaker+ myomerger+ fibroblasts but not empty-infected myomaker+ fibroblasts. Arrows indicate fusion between GFP+ and NLS-Tom+ fibroblasts. The percentage of nuclei in syncytia after expression of empty or myomerger (n=3). **c**, Heterologous fusion experiment between C2C12 myoblasts and GFP+ fibroblasts infected with either empty, myomaker, or myomerger. Representative immunofluorescent images to visualize co-localization of myosin and GFP (arrows), indicating fusion. Quantification of the percentage of GFP+ myosin+ cells (n=3). Data are presented as mean ± SEM. *P<0.05 compared to empty. #P<0.05 between myomaker and myomerger. Scale bars, 50 μm (**a**, **b**), 100 μm (**c**).
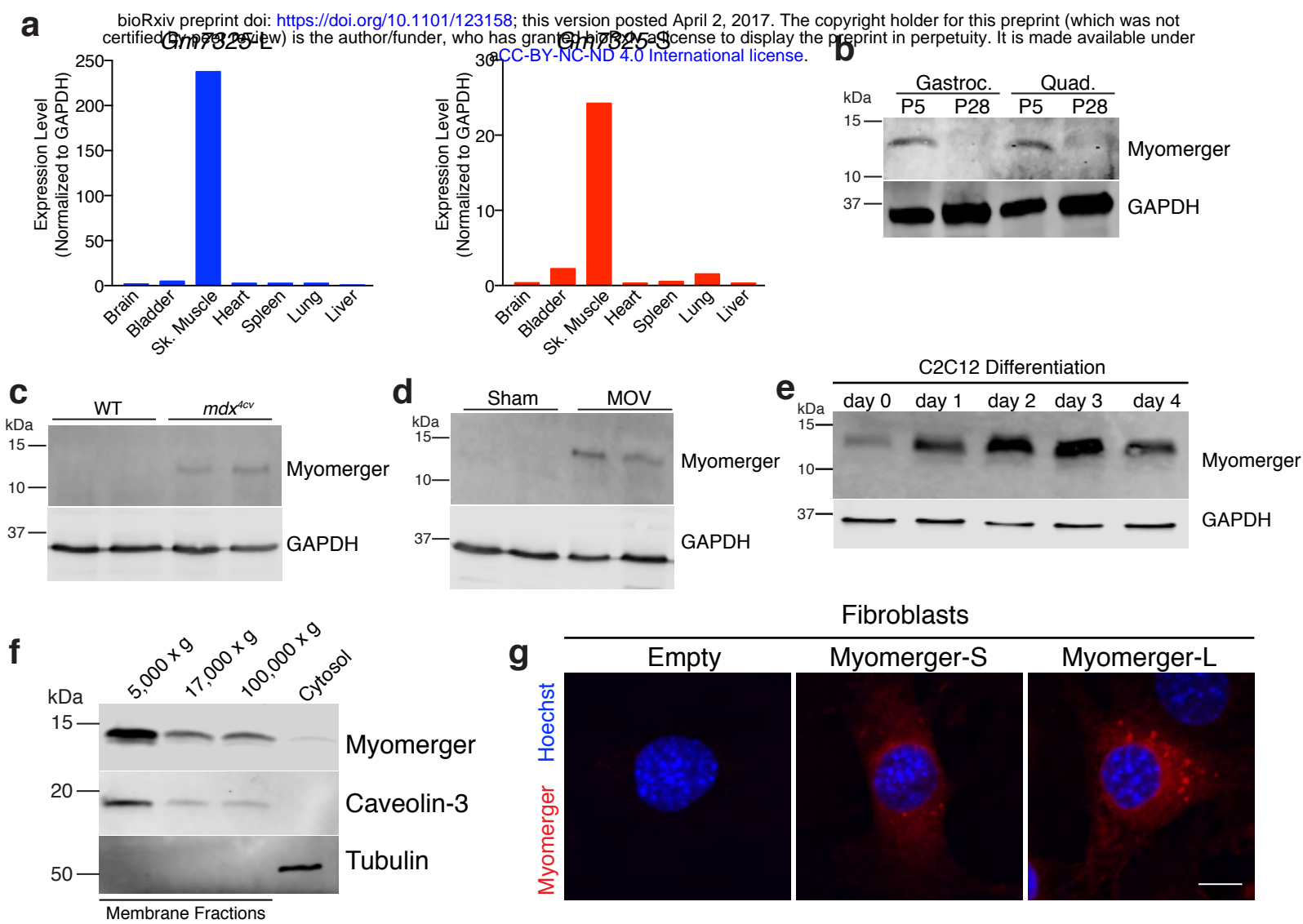
Figure 2. Muscle-specific expression and regulation of myomerger. a, qRT-PCR for both *Gm7325* long (L) and short (S) transcripts from various postnatal (P) day 5 tissues. **b-e**, Immunoblotting for myomerger comparing P5 muscle to P28 muscle (**b**), WT to *mdx⁴ᶜᵛ* diaphragms (**c**), sham plantaris to mechanically overloaded (MOV) plantaris (**d**), and during C2C12 myoblast differentiation (**e**). GAPDH was used as a loading control. **f**, Fractionation of C2C12 lysates on day 2 of differentiation followed by immunoblotting. **g**, Representative immunostaining of fibroblasts infected with either empty, myomerger-short (S), or myomerger-long (L). Scale bar, 10 µm.
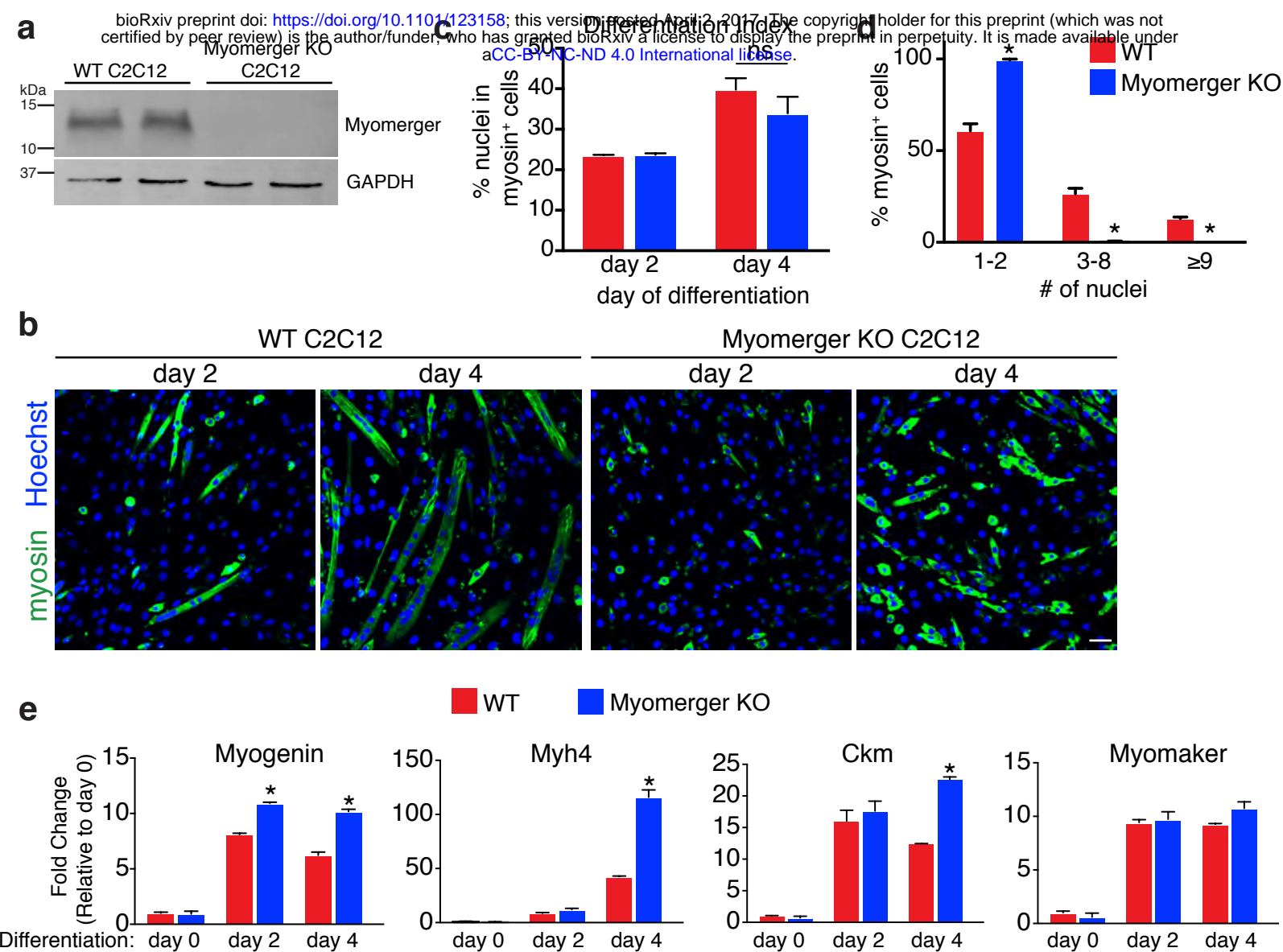
Figure 3. Requirement of myomerger for myoblast fusion *in vitro*. a, Immunoblotting for myomerger in WT and myomerger KO C2C12 cells on day 2 of differentiation. GAPDH was used as a loading control. **b**, Representative immunofluorescence images on day 2 and day 4 of differentiation for WT and myomerger KO C2C12 cells. Myomerger KO cells differentiate but fail to fuse. **c**, Quantification of the differentiation index, the percentage of nuclei in myosin+ cells (*n*=4). ns, not significant. **d**, The percentage of myosin+ cells that contain 1-2, 3-8, or ≥9 nuclei after 4 days of differentiation, as an indicator of fusogenicity (*n*=3). **e**, qRT-PCR for the indicated myogenic transcripts (*n*=4). Data are presented as mean ± SEM. *$P<0.05$ compared to WT. Scale bar, 50 μm.
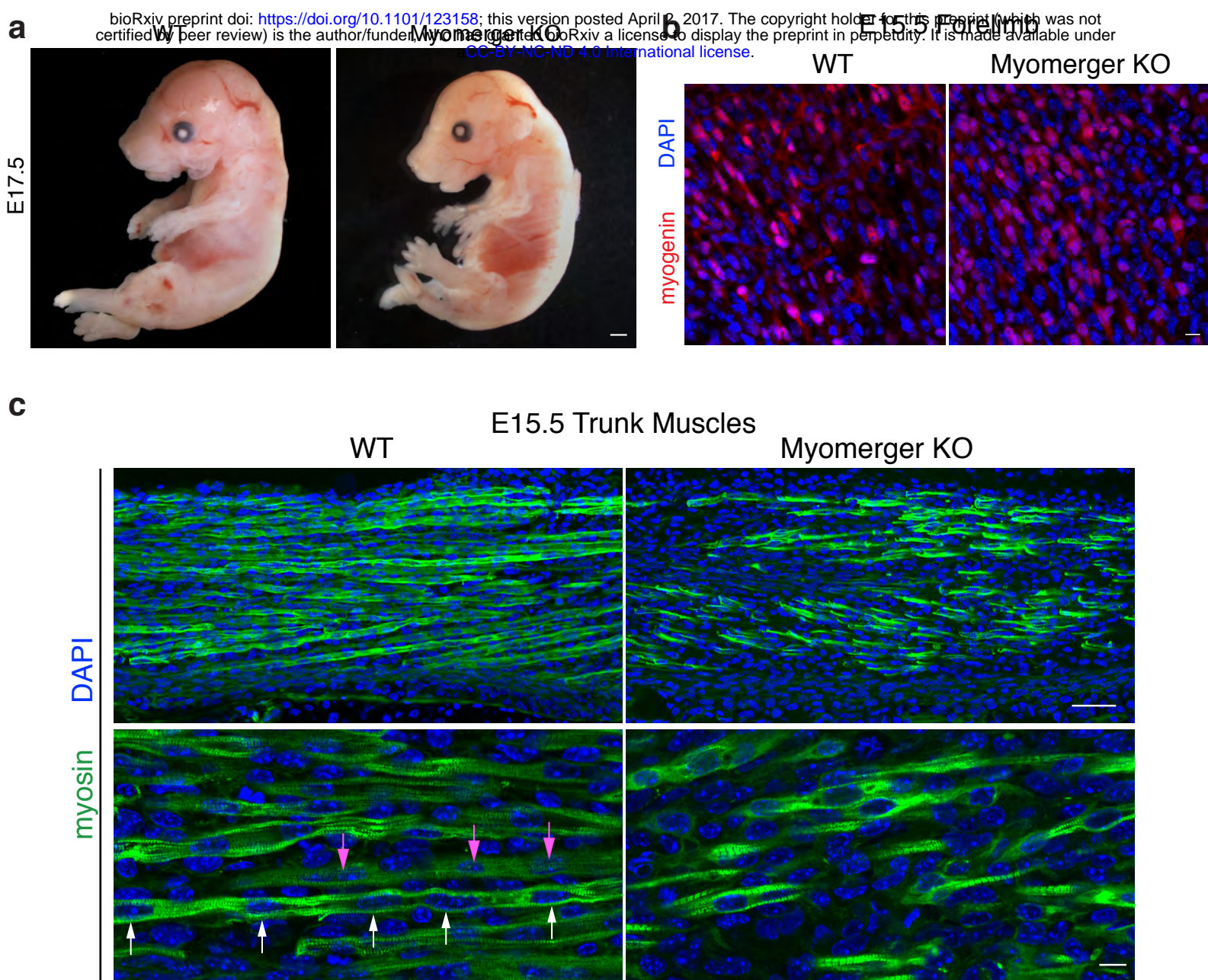
Figure 4. Myomerger is essential for myoblast fusion and muscle formation during embryonic development. a, Representative whole-mount images of WT and myomerger KO E17.5 embryos showing improper skeletal muscle formation in KO embryos (*n*=4). **b**, Immunofluorescence images for myogenin from WT and myomerger KO E15.5 forelimbs demonstrating that myomerger is not required for myogenic activation (*n*=3). **c**, Myosin immunofluorescence on the indicated E15.5 trunk muscles (*n*=3). Multi-nucleated myofibers (arrows of same color show nuclei within one myofiber) were observed in WT sections. Myomerger KO myocytes were myosin+ with sarcomeres but remained mono-nucleated. Scale bars, 1 mm (**a**), 50 μm (**c**, top panels), 10 μm (**b, c**, bottom panels).
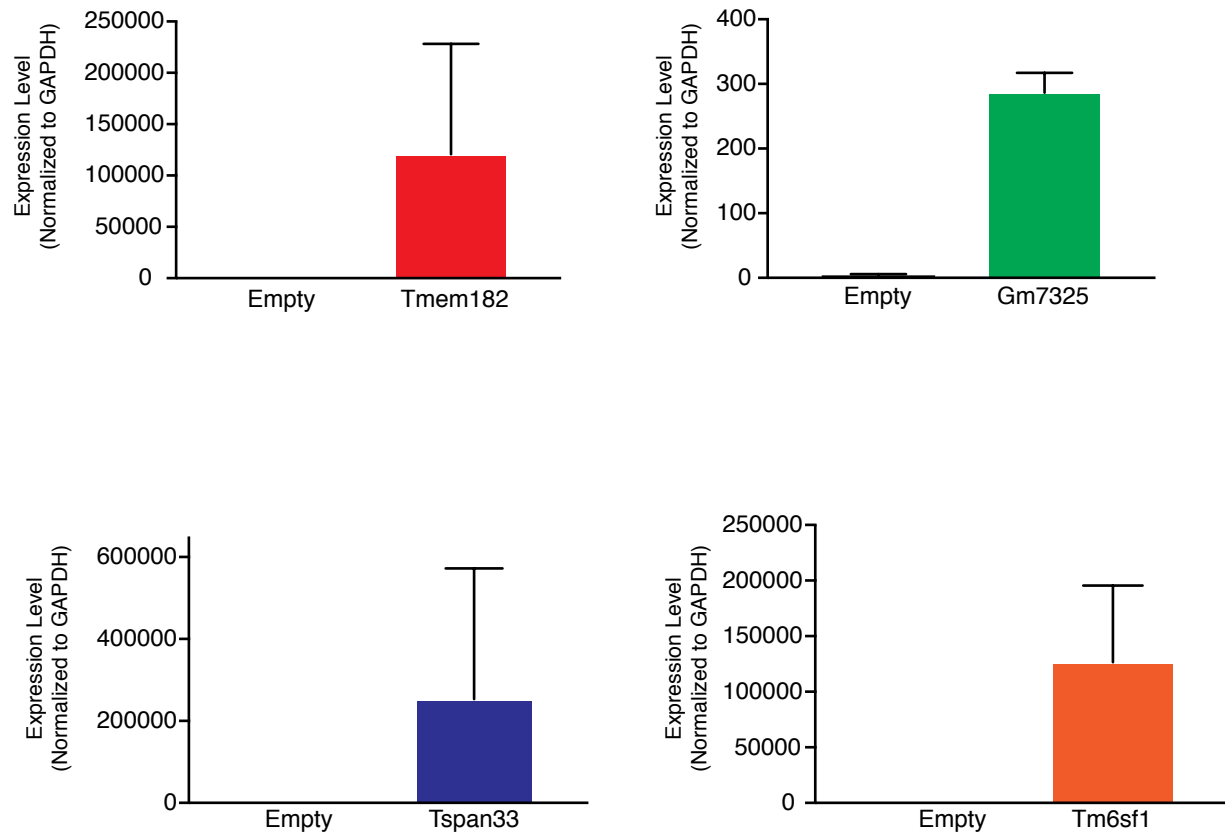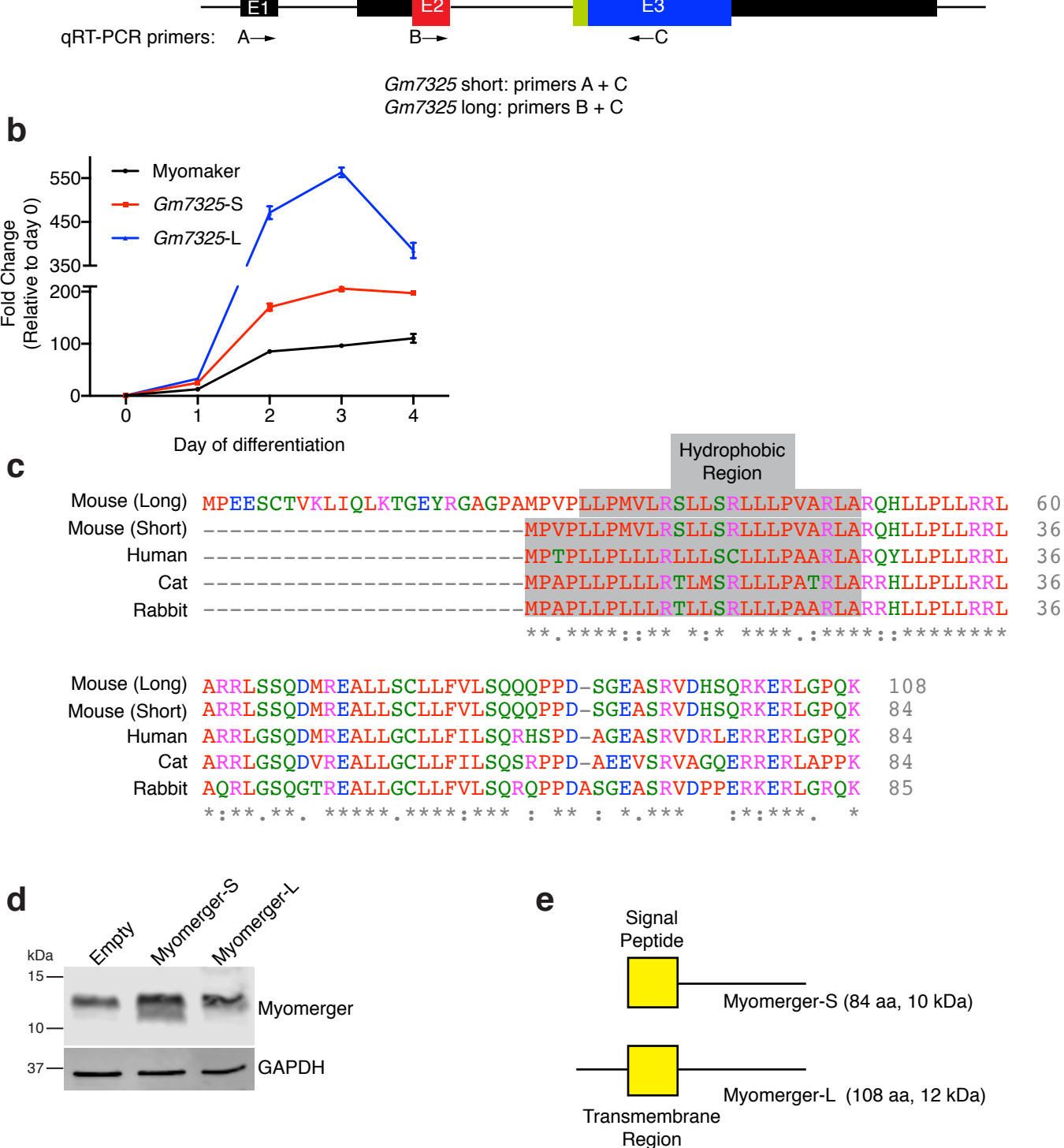
Extended Data Figure 1. Expression of MyoD-regulated genes in myomaker⁺ fibroblasts. qRT-PCR analysis for the indicated genes 72 hours after expression in fibroblasts. For *Gm7325*, we used primers specific for the long transcript.
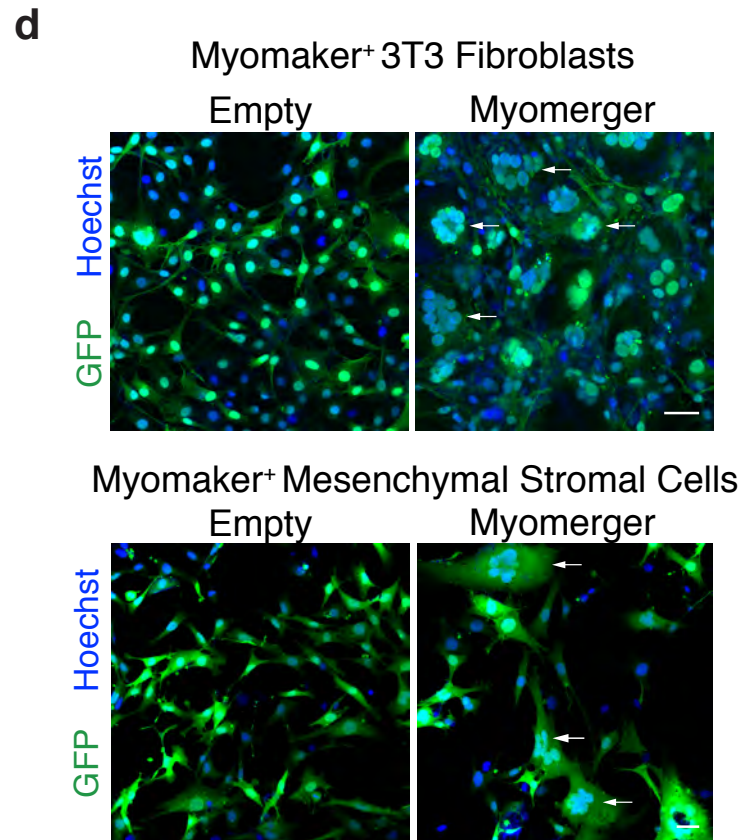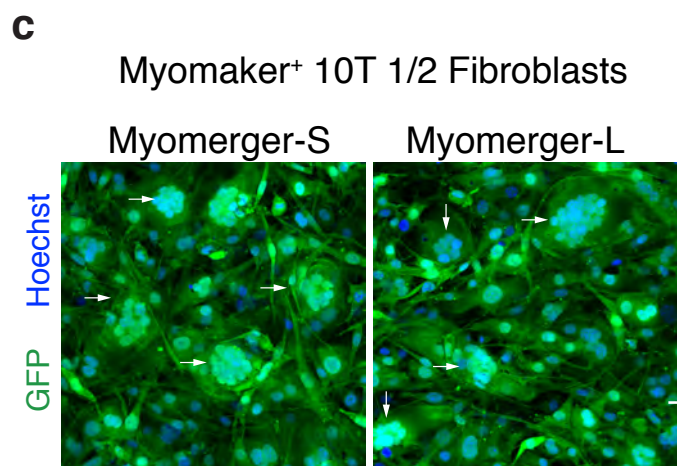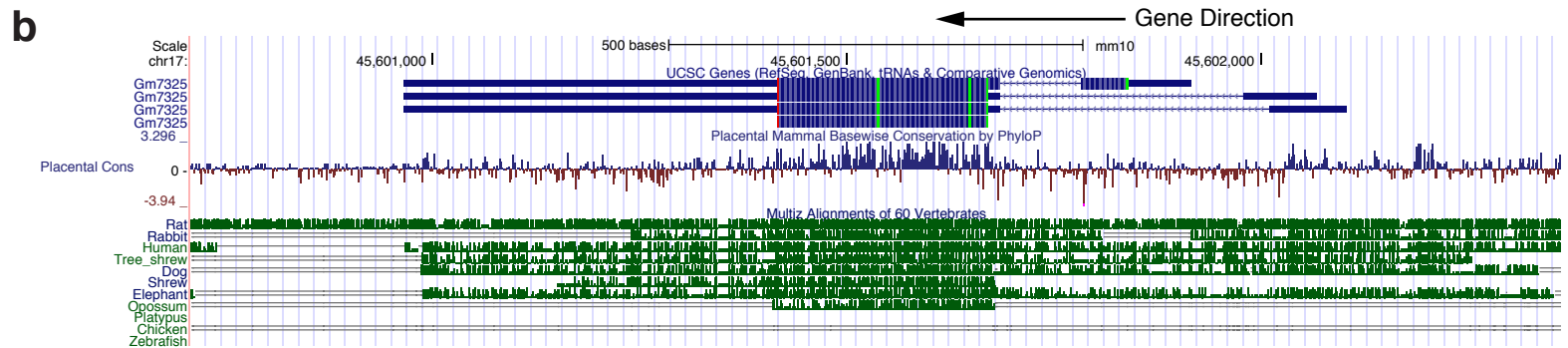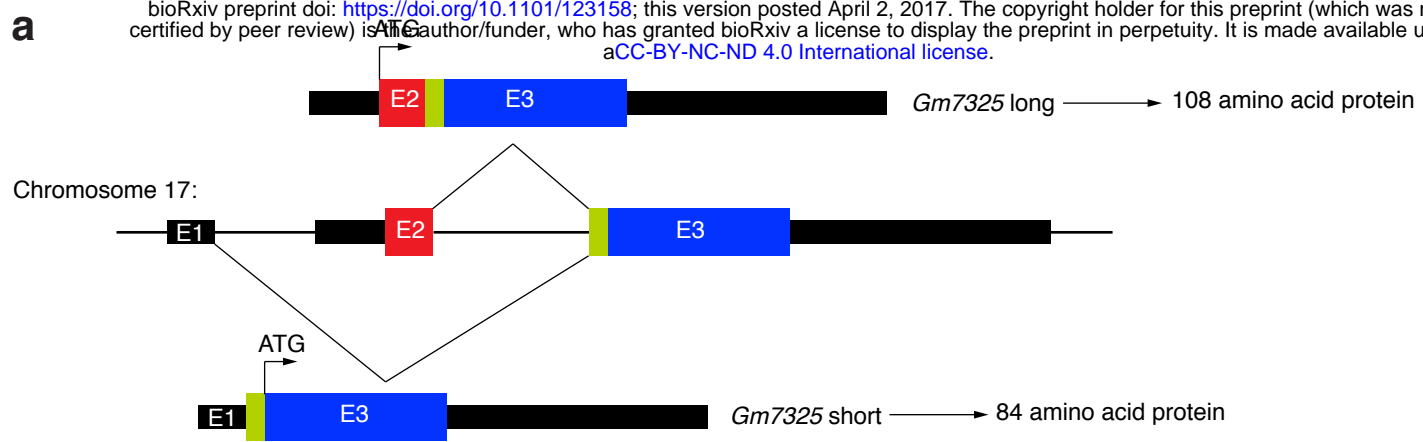
Extended Data Figure 2. Genomic organization of murine *Gm7325* and the ability of both variants to induce fusion. a, Diagram showing the Gm7325 locus on chromosome 17. The short transcript is generated by splicing of exon 1 (non-coding) with exon 3, leading to an 84 amino acid protein. The long transcript is produced by splicing of exon 2 with exon 3 and results in a 108 amino acid protein. **b**, UCSC genome browser track showing multiple transcripts and conservation across vertebrate species. The short transcript is highly conserved in multiple species, including human, but not present in zebrafish. The upstream exon that produces the longer transcript is not highly conserved. Note that this annotation displays the gene on the reverse strand. **c**, The short (S) or long (L) myomerger transcripts were expressed in myomaker+ 10T ½ fibroblasts and both induced fusion (n=3). **d**, Myomerger also induced fusion of myomaker+ NIH/3T3 fibroblasts (n=3) and myomaker+ mesenchymal stromal cells (n=3). Arrows indicate fusion. Scale bars, 50 μm.
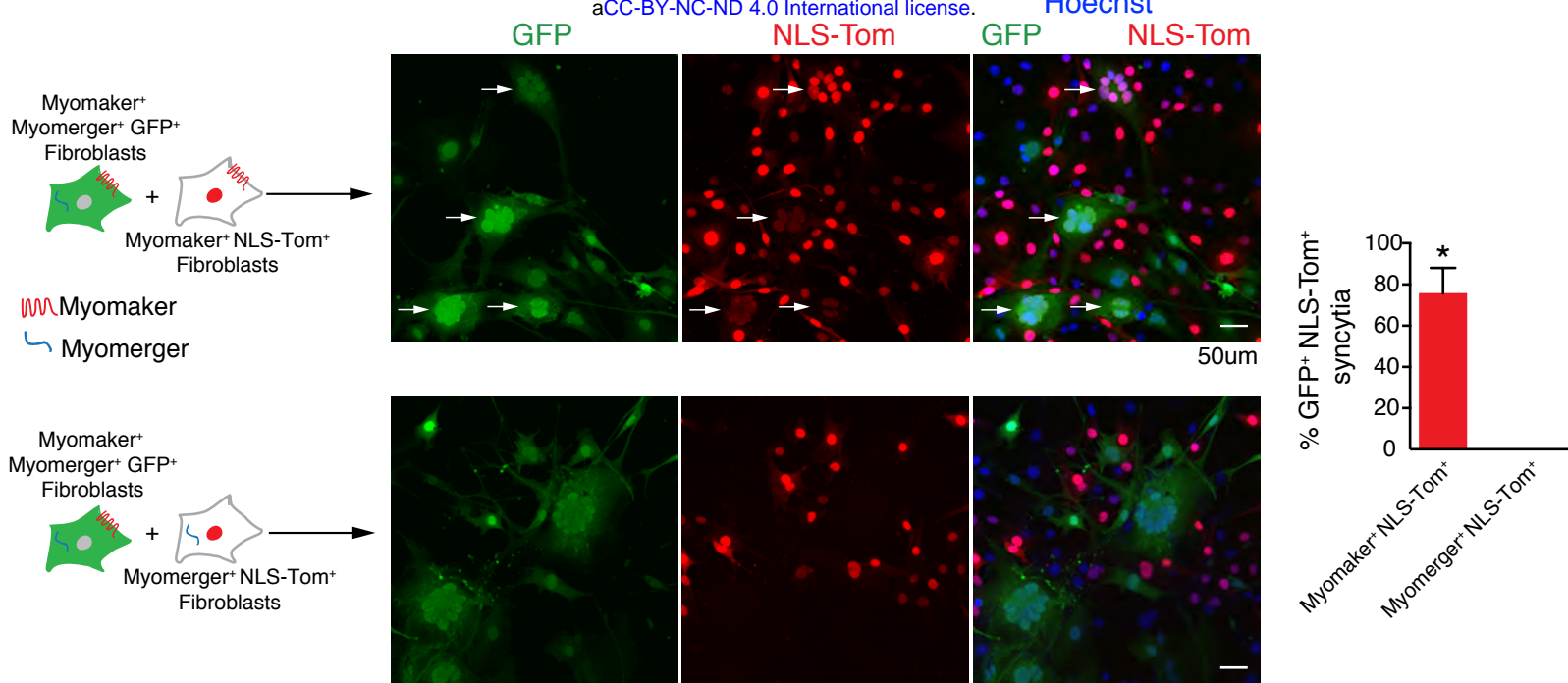
Extended Data Figure 3. Efficient fusion requires myomaker expression in both fusing cells but myomerger in one fusing cell. Diagram showing the cell mixing approach to assess fusion between the populations of fibroblasts. Co-localization of GFP and NLS-TdTomato (NLS-Tom) in the nucleus represents fusion (arrows). Representative images demonstrate fusion of myomaker+ myomerger+ GFP+ fibroblasts with myomaker+ NLS-Tom+ fibroblasts but not myomerger+ NLS-Tom+ fibroblasts. The percent of GFP+ NLS-Tom+ syncytia (*n*=3). Data are presented as mean ± SEM. *P<0.05 compared to myomerger+ NLS-Tom+ fibroblasts. Scale bars, 50 μm.

a

E1　E2　E3

qRT-PCR primers:　A→　B→　←C

Gm7325 short: primers A + C
Gm7325 long: primers B + C

b

c

Mouse (Long)	MPEESCTVKLIQLKTGEYRGAGPAMPVPLLPMVLRSLLSRLLLPVARLARQHLLPLLRRL	60
Mouse (Short)	------------------------MPVPLLPMVLRSLLSRLLLPVARLARQHLLPLLRRL	36
Human	------------------------MPTPLLPLLLRLLLSCLLLPAARLARQYLLPLLRRL	36
Cat	------------------------MPAPLLPLLLRTLMSRLLLPATRLARRHLLPLLRRL	36
Rabbit	------------------------MPAPLLPLLLRTLLSRLLLPAARLARRHLLPLLRRL	36
	.***:.** *.* ****.:*****::*********	

Mouse (Long)	ARRLSSQDMREALLSCLLFVLSQQQPPD-SGEASRVDHSQRKERLGPQK	108
Mouse (Short)	ARRLSSQDMREALLSCLLFVLSQQQPPD-SGEASRVDHSQRKERLGPQK	84
Human	ARRLGSQDMREALLGCLLFILSQRHSPD-AGEASRVDRLERRERLGPQK	84
Cat	ARRLGSQDVREALLGCLLFILSQSRPPD-AEEVSRVAGQERRERLAPPK	84
Rabbit	AQRLGSQGTREALLGCLLFVLSQRQPPDASGEASRVDPPERKERLGRQK	85
	*:**.**. *****.****:*** : ** : *.*** :*:***. *	

d

e

Signal Peptide

Myomerger-S (84 aa, 10 kDa)

Myomerger-L (108 aa, 12 kDa)

Transmembrane Region

**Extended Data Figure 4. Design of qRT-PCR primers and comparison of myomerger protein variants.** **a**, Schematic showing the location of primers to distinguish short and long transcripts. **b**, qRT-PCR for *Gm7325* transcript variants and myomaker in C2C12 cells on the indicated days of differentiation (*n*=3 for each time point). **c**, Sequence alignment of both mouse myomerger protein products with multiple mammalian orthologs using Clustal Omega. A potential hydrophobic region is highlighted in gray. **d**, Immunoblotting from C2C12 cells infected with either empty, myomerger-short (S), myomerger-long (L) on day 2 of differentiation. Myomerger migrates as a single band around 12 kDa when endogenously produced (empty). Over-expression of myomerger-S leads to an increase in the endogenous band and a lower band is also detected suggesting that myomerger transcripts may be subjected to intricate mRNA processing or post-translational modifications. **e**, Graphic showing the regions of myomerger-S and myomerger-L as predicted by SignalP and Phobius.
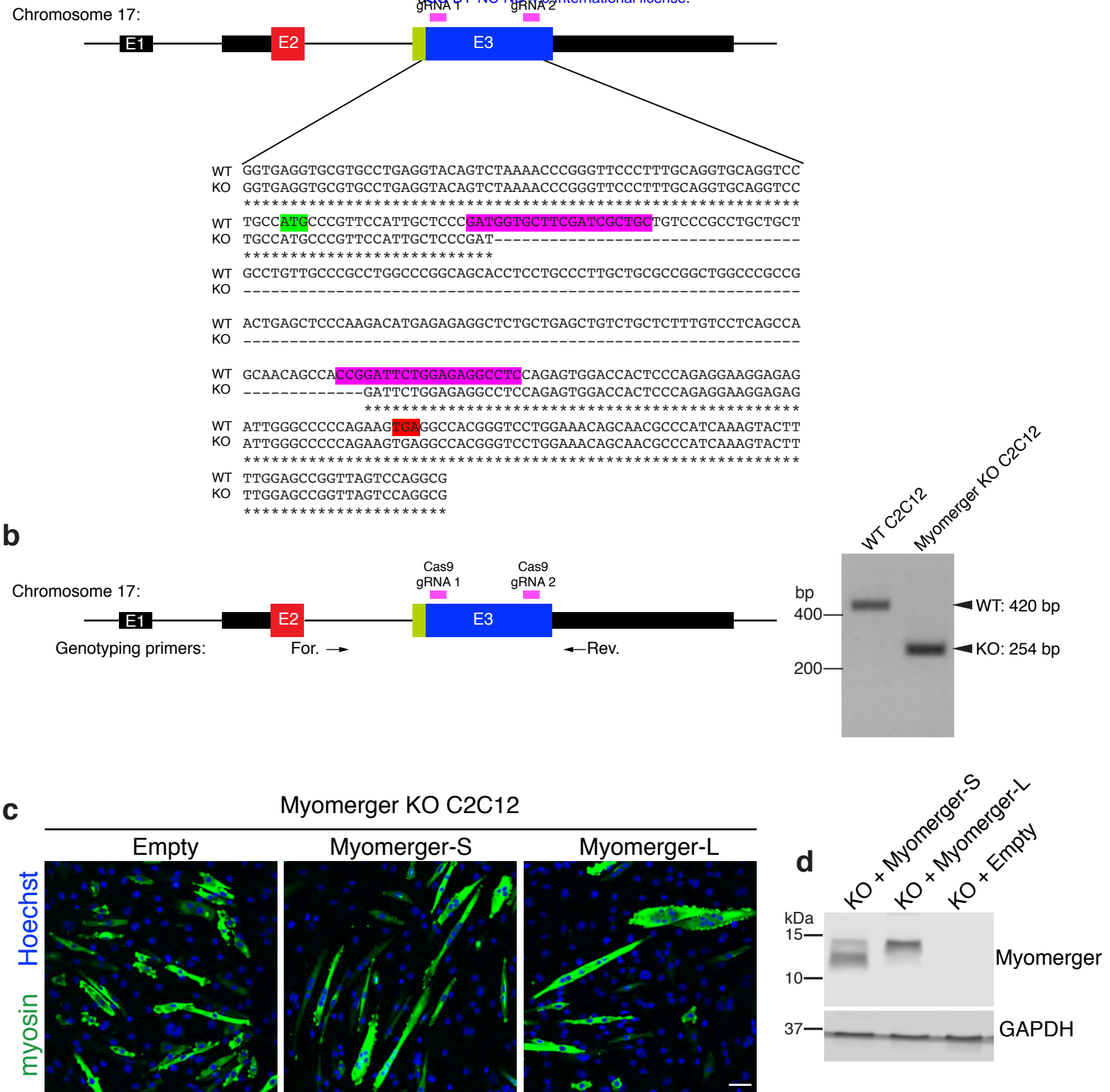
Extended Data Figure 5. CRISPR/Cas9 disruption of the *Gm7325* locus. **a**, Schematic showing the Gm7325 locus and targeting of sgRNAs. **b**, Genotyping strategy for myomerger KO C2C12 cells. WT and KO PCR products were sequenced and the result is shown below the diagram in (**a**). The use of two sgRNAs results in reproducible cut sites leading to a 166 base pair deletion in both C2C12 cells and mice. The translational start site (ATG, green) for myomerger-S and stop site (TGA, red) for both myomerger-S and myomerger-L are noted. **c**, Myomerger KO C2C12 cells were infected with either empty, myomerger-S, or myomerger-L and induced to differentiate. Both myomerger-S and myomerger-L rescued the lack of fusion in myomerger KO cells. **d**, Immunoblotting for myomerger shows appropriate expression after transduction of myomerger KO cells. Scale bars, 50 μm.
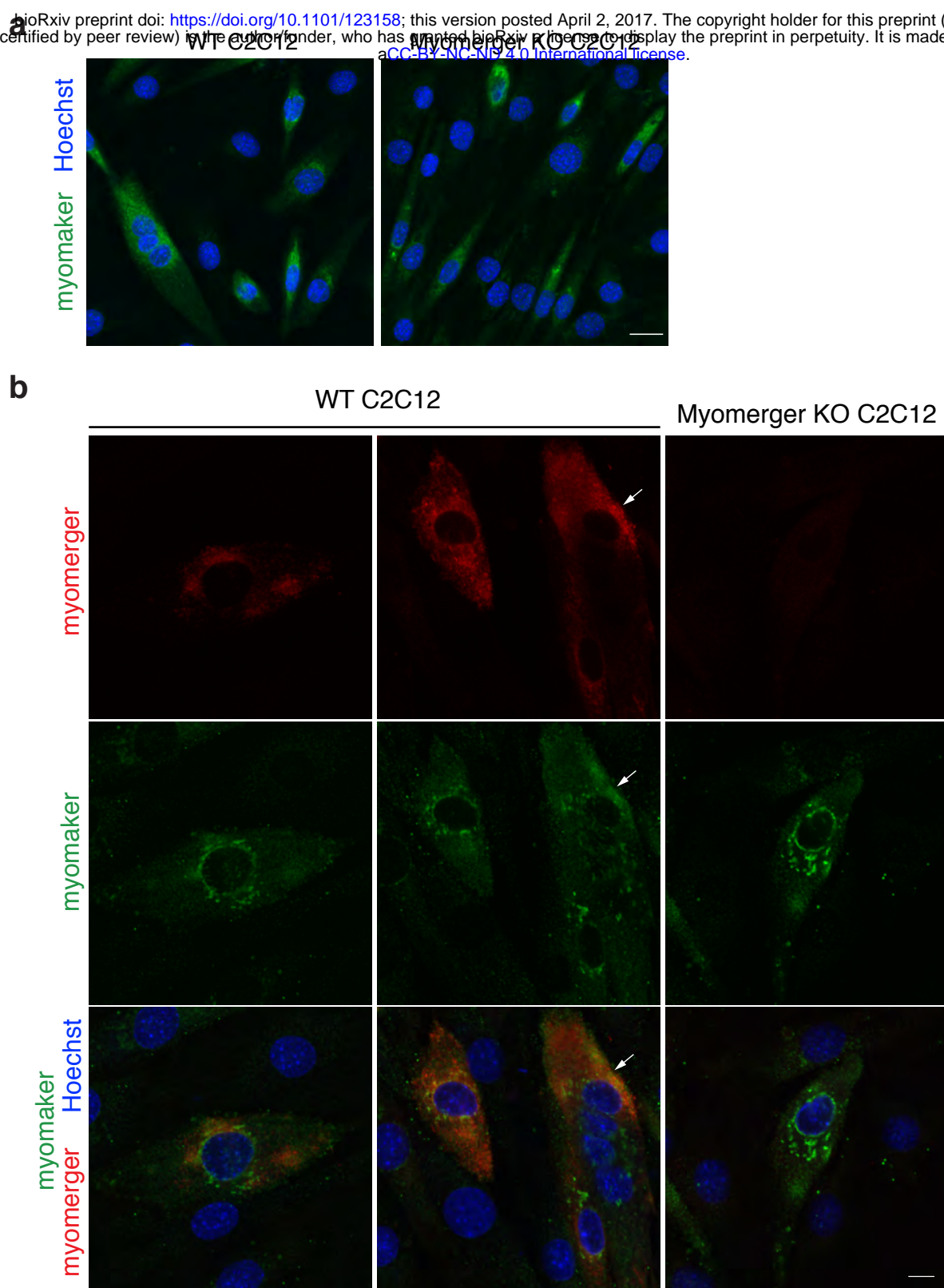
Extended Data Figure 6. Analysis of myomaker and myomerger co-localization. **a**, Representative immunofluorescence images from WT and myomerger KO C2C12 cells on day 2 of differentiation indicating that loss of myomerger does not alter myomaker expression or localization. **b**, Immunofluorescence for myomerger and myomaker on the indicated cells on day 2 of differentiation. These two fusion proteins exhibit different patterns, although modest co-localization (arrows) was observed. The functional significance of this potential co-localization is not currently known. Scale bars, 10 µm (**a**), 5 µm (**b**).
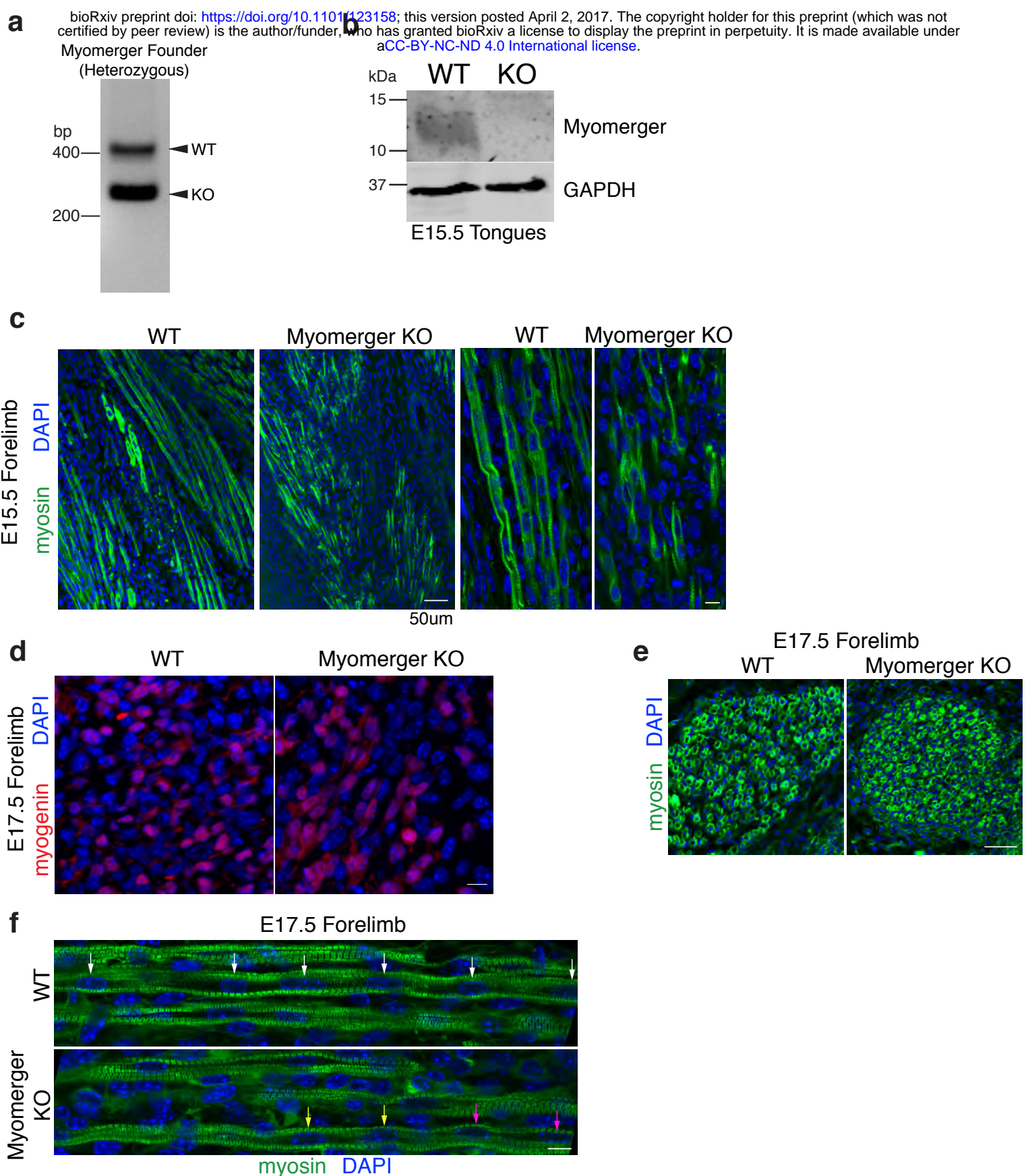
Extended Data Figure 7. Examination of myomerger KO muscle. **a**, Genotyping of the one founder harboring the *Gm7325* mutation generated through Cas9-mutagensis. **b**, Immunoblotting on tongue lysates from WT and myomerger KO mice showing lack of myomerger in KO samples. GAPDH was used as a loading control. **c**, E15.5 forelimbs (*n*=3) immunostained with a myosin antibody demonstrates that myomerger KO myoblasts differentiate but are unable to fuse. **d-e**, E17.5 forelimbs from WT and myomerger KO mice were evaluated for myogenin and myosin expression, and multi-nucleation. Arrows of same color in (**f**) show nuclei within one myofiber. We observed myocytes in myomerger KO samples that contained two nuclei (arrows). Analysis of z-stack images (not shown) indicated that the nuclei labeled by the yellow and pink arrows are not within the same myofiber. Scale bars, 50 μm (**c,** left panels, **e**), 10 μm (**c**, right panels, **d**, **f**).